Available online at www.sciencedirect.com
SCIENCE DIRECT®
International Journal of Thermal Sciences 45 (2006) 962–968
International Journal of Thermal Sciences
www.elsevier.com/locate/ijts

Characterization of the effect of surface roughness and texture on fluid flow—past, present, and future ☆

James B. Taylor [a,*], Andres L. Carrano [b], Satish G. Kandlikar [c]

[a] *Industrial & Systems Engineering, Micro Systems Engineering, Rochester Institute of Technology, 81 Lomb Memorial Dr., Rochester, NY 14623, USA*
[b] *Industrial & Systems Engineering, Rochester Institute of Technology, Rochester, NY 14623, USA*
[c] *Mechanical Engineering, Micro Systems Engineering, Rochester Institute of Technology, Rochester, NY 14623, USA*

Received 10 September 2005; accepted 10 January 2006

Available online 13 February 2006

Abstract

Surface roughness (texture) has an effect on fluid flow in networks which has been studied for well over a century. The exact effect roughness has on fluid flow has not been completely understood, but a working estimate has been offered by a variety of authors over time. The work of Colebrook, Nikuradse, and Moody has provided practitioners with a method to include at least a first order estimate of roughness effects, but their work has been limited to relative roughness (roughness height to diameter) values of 5% or less. Modern fluidic systems at the mini- and micro-levels routinely violate the 5% relative roughness threshold due to the inability to control the roughness of surfaces to sufficient levels with respect to decreasing system scale. Current work by Kandlikar et al., has extended the traditional methods of assessing surface roughness effects up to 14% relative roughness by including the effect of constricted flow diameters (modified flow diameter based on constrictions caused by surface roughness) and modifying the Moody diagram to reflect new experimental data. The future of micro fluidics would suggest that trends for miniaturization will continue and that further understanding and experimentation will be warranted. This is especially true with regards to understanding the role of roughness on the flow in mini- and micro-channels.

Keywords: Roughness; Micro-fluidics; Single phase flow; Micro-channels

1. Introduction

This paper seeks to lay out the historical understanding of the effects of surface roughness and texture on fluid flow. A historical perspective is reviewed as well as current understanding. Changes to the present method to accommodate the decreasing size of fluidic systems at the mini- and micro-levels have been proposed to extend the applicability from 5% relative roughness to diameter values to 14%. The future of fluid flow and the increasing effect of roughness are explored in a section at the end of this paper. Several potential methods for improving the understanding of and controlling the effect of surface roughness and texture are explored.

2. Past

2.1. Pioneers

Pressure drop during internal flow is one of the most important considerations in designing a fluid flow system. Surface roughness was identified as an important parameter in fluid flow as early as in the nineteenth century by Darcy [1], who carefully conducted experiments with pipes of varying roughness. Darcy's work introduced the concept of surface roughness to the science of fluid dynamics and fluid flow. Fanning [2] proposed a correlation for the pressure drop and surface roughness in the design of hydraulic flow in networks. The pioneering work on understanding the effect of roughness on pressure drop was done by Nikuradse [3]. He coated the inside walls of pipes with uniform sand grains of known sizes using Japanese lacquer.

☆ A preliminary version of this paper was presented at ICMM05: Third International Conference on Microchannels and Minichannels, held at University of Toronto, June 13–15, 2005, organized by S.G. Kandlikar and M. Kawaji, CD-ROM Proceedings, ISBN: 0-7918-3758-0, ASME, New York.

* Corresponding author. Tel.: +1 585 475 6185; fax: +1 585 475 2520.
E-mail address: james.taylor@rit.edu (J.B. Taylor).

1290-0729/$ – see front matter
doi:10.1016/j.ijthermalsci.2006.01.004

Nomenclature

b	channel base
b_{cf}	constricted channel height based on ridge height
$b_1, b_2, \ldots$	roughness bearing length
B	bias error
C	laminar friction factor constant used to calculate f
D_{cf}	constricted tube diameter
D_h	hydraulic diameter
$D_{h,\mathrm{cf}}$	constricted flow hydraulic diameter
D_t	tube root diameter
f	Fanning friction factor
f_{cf}	Fanning friction factor, constricted flow diameter
f_{Moody}	Moody friction factor, $= 4f$
$f_{\mathrm{Moody,cf}}$	modified Moody friction factor, constricted flow diameter
F_p	floor distance to mean line
l	channel length
$\dot{m}$	mass flow rate ..... kg s^{-1}
p	pitch
P	pressure ..... Pa
P_e	precision error
P_c	peak density
Ra	average roughness
Re	Reynolds number based on D_t
Re_{cf}	Reynolds number based on $D_{h,\mathrm{cf}}$ or D_{cf}
R_{ku}	kurtosis
R_p	maximum profile peak height
R_q	root mean square roughness
R_{sk}	skewness
R_{sm}	mean spacing of profile irregularities
R_t	maximum height between irregularities
R_v	maximum height of valley below mean
R_y	peak roughness
R_z	average maximum height of profile
S_m	spacing between irregularities
t_p	profile bearing length ratio
w	channel width
x	distance from channel entrance
Z	profile height from the mean

Greek letters

α	aspect ratio of the rectangular channel
ε	roughness height
ε/D_t	relative roughness based on root diameter
$\varepsilon/D_{\mathrm{cf}}$	relative roughness, constricted flow diameter
μ	viscosity ..... Ns m^{-2}

Subscripts

cf	constricted flow
fd	fully developed
h	hydraulic

The pipe diameters were 25, 50 and 100 mm and the Reynolds numbers employed were from 600 to 10^6. Colebrook [4] later performed experiments on sixteen spun concrete-lined pipes and six spun bitumastic-lined pipes ranging in diameter from 101.6 mm to 1524 mm with average surface roughness values between 0.04318 mm and 0.254 mm. He also tested the 5486 mm diameter Ontario tunnel, which was a concrete tunnel made from steel oil forms. The resulting pressure drop data was correlated with his well-known Colebrook equation:

$$\frac{1}{f_{\mathrm{Darcy}}^{0.5}} = -2.0\log\left(\frac{\varepsilon/D_t}{3.7} + \frac{2.51}{Re\, f_{\mathrm{Darcy}}^{0.5}}\right) \quad (1)$$

Moody [5] presented Colebrook's results in a graphical format in his well-known Moody diagram. He plotted the Darcy friction factor f_{Darcy} as a function of Reynolds number over a relative roughness (ε/D_t) range of 0 to 0.05. The plot covered the laminar as well as the turbulent region.

In the laminar region, the roughness was shown to have very little effect, but in the turbulent region, roughness played a major role. The friction factor increased with Reynolds number and asymptotically reached a constant value at higher Reynolds numbers. The constant asymptotic value of the friction factor increased with increasing relative roughness.

2.2. Traditional measures of surface roughness

Surfaces represent the object boundary where most interactions take place. In a manufacturing environment, the creation of surface textures is generally the consequence of complex interactions between processes and materials, among others. Since these textures will determine, to a large degree, surface behavior and performance, control of the processes that produce them as well as accurate characterization of their geometries and irregularities is of utmost importance.

Surface texture is the composite profile of certain deviations that are typical of a real surface. These include:

- *Roughness*: the finer irregularities of surface texture that are inherent in the materials or production process, i.e. cutting tool, spark, grit size, etc.
- *Waviness*: the more widely spaced component of surface texture and upon which roughness is superimposed. It may result from vibrations, chatter, etc.
- *Error of form*: the general shape of the surface neglecting roughness and waviness. It generally consists of the departure from the intended shape. It may be caused by lack of machine rigidity, etc.

Modern surface finish measurement traces back to the stylus techniques developed in the 1930's, where a small tip is moved across a surface while vertical deflections are recorded. A series of 2D parameters aimed at describing various surface characteristics (such as peak to valley, rms, etc.) have been developed since and documented in several standards [6–9]. However, despite the breadth of available surface parameters, common in-

dustry practice is to specify and control surfaces with a single indicator, generally the mathematical average roughness (*Ra*). The reasons for such practice are several: average roughness is easy to measure and calculate, it is well established and understood with literature and standards available to explain it, and, perhaps more importantly, historical surface data is often based upon it. Scientists and engineers know that they can specify *Ra* and achieve a surface finish within that specification. This knowledge is typically based on the experience the designers have with various processes and manufacturing techniques as well as the roughness specifications and machine capability.

Often times, experience has shown, one number is not enough to describe the complete functionality of a surface or its interface. A surface with sharp spikes, deep pits, or general isotropy may all yield the same average roughness value while performing extraordinarily differently. *Ra* makes no distinction between peaks and valleys nor does it provide information about spatial structure. While *Ra* remains useful as a general guideline on the surface texture, it has been shown to be too general to describe the surface's functional nature in today's ever increasing complexity of applications.

Over time, hundreds of different parameters have been developed to address the shortcomings that arise from use of a single parameter. These have been broadly classified into: roughness and waviness height, spacing and amplitude, shape, as well as aerial parameters. Also, more sophisticated instrumentation has been providing information on surface texture in different format and resolution. This has been possible due to the incorporation of optical and non-contact methods such as white light interferometry, laser based triangulation, atomic force microscopy, scanning electron microscopy and confocal optical microscopy to name a few.

2.3. Nikuradse and surface roughness

The pioneering work on characterizing the effect of surface roughness on pressure drop by Nikuradse is the foundation for the Moody diagram that pertains to pipes that have relatively low values of relative surface roughness. The underlying data in this diagram was developed by using sand grains to induce a known roughness on the inside surfaces of pipes. Consequently, this diagram is used extensively in predicting friction factors for commercial tubes whose roughness features are not too different from the sand grain roughness. This work provided the foundations for establishing the effects of relative roughness (ε/D) on flow characteristics, but, as the relative roughness becomes large (>5%), it becomes important to consider additional roughness features as well.

The initial characterization of surface roughness by Nikuradse was limited to the diameter of the sand grain (equivalent to the modern descriptor *Average Maximum Height of the Profile,* R_z) and did not consider other parameters that would describe the spacing, waviness, and shape in a three-dimensional area profiling. Additionally, when considering mini-channels (3 mm $\geqslant D_h >$ 200 μm) and micro-channels (200 μm $\geqslant D_h >$ 10 μm) [10], the ratio between the hydraulic diameter and the geometry of the roughness profile becomes significantly different from those in conventional channels. At this scale, the shape, spacing and size of the roughness irregularities have different influence upon the pressure drop and the overall fluid flow characteristics. In particular, for high values of relative roughness, the flow over roughness features induces recirculation and flow separation and is expected to play a role in single-phase pressure drop. There is clearly a need for developing a set of roughness descriptors suitable for micro-channels and mini-channels that would allow for a better understanding of the effects of different aspects of surface topography upon the pressure drop and fluid flow behavior.

3. Present

3.1. Constricted flow effects

Kandlikar et al. [11] considered the effect of flow constriction due to roughness elements and proposed that the constricted flow area be taken in the velocity calculations. Accordingly, the Reynolds number and the friction factors were redefined based on the constricted flow diameter, defined as follows:

$$D_{\mathrm{cf}} = D_t - 2\varepsilon \tag{2}$$

where D_{cf} is the constricted flow diameter, D_t is the tube diameter (root), and ε is the surface roughness. The friction factor using the constricted flow diameter is related to the friction factor based on the root diameter as given by the following equation:

$$f_{\mathrm{Darcy,cf}} = f_{\mathrm{Darcy}}\left[\frac{D_t - 2\varepsilon}{D_t}\right] \tag{3}$$

In the laminar region, the Darcy friction factor for a circular pipe was defined based on the Reynolds number calculated using the constricted flow diameter:

$$f_{\mathrm{Darcy,cf}} = \frac{64}{Re_{\mathrm{cf}}} \tag{4}$$

In the turbulent region, the Colebrook equation is expressed in terms of the constricted flow diameter as follows:

$$\frac{1}{\left(\frac{D_t}{D_t-2\varepsilon}\right)^{2.5} f_{\mathrm{Darcy,cf}}^{0.5}} = -2.0\log\left(\frac{\varepsilon/D_t}{3.7} + \frac{2.51}{Re_{\mathrm{cf}}\left(\frac{D_t}{D_t-2\varepsilon}\right)^{3.5} f_{\mathrm{Darcy,cf}}^{0.5}}\right) \tag{5}$$

The Moody diagram is replotted by Kandlikar et al. [11] using the above equations and is shown in Fig. 1.

Several interesting features may be noted in Fig. 1. In the turbulent region, a distinct difference is noted from the original Moody diagram. The higher roughness plots in the fully rough region (corresponding to high Reynolds numbers) reach a plateau around 0.042 beyond $\varepsilon/D_t > 0.03$. In other words, $f_{\mathrm{Darcy,cf}} = 0.042$ for $0.03 \leqslant \varepsilon/D \leqslant 0.05$. Recall that the highest value of relative roughness covered in the Moody diagram is 0.05. Since no experimental data is available beyond $\varepsilon/D_t >$ 0.05, the applicability of the above plot to the higher relative roughness values cannot be ascertained.

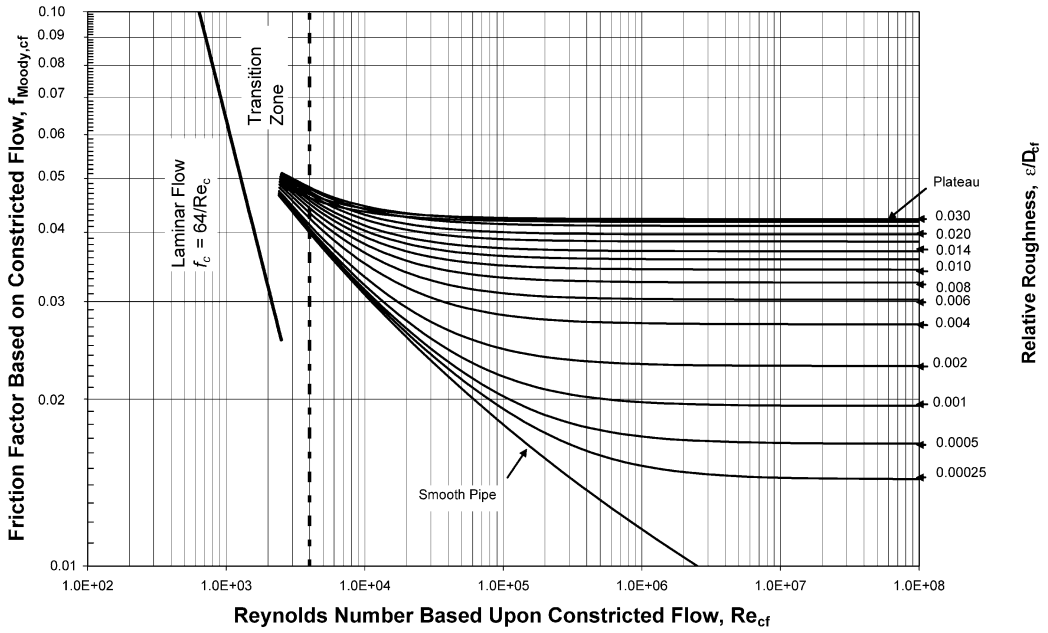

Fig. 1. Moody diagram based on the constricted flow diameter, Kandlikar et al. [11].

In the laminar region, the plot shows a similar relation between the constricted friction factor and the Reynolds number as displayed in the Moody diagram. This needs further validation, as the available experimental data in this region is available only for small values of relative roughness. Further, the difference between the original Moody plot and the modified plot is quite small for relative roughness values of less than 0.05.

In an attempt to verify the applicability of the modified Moody plot in the laminar region, Kandlikar et al. [11] and Schmitt and Kandlikar [12] conducted experiments with structured roughness features. They tested aligned and offset sawtooth roughness structures as shown in Fig. 2 with ε/D_t as high as 0.14. A 10.03 mm wide rectangular channel with a variable gap arrangement was employed. The gap height was varied to yield hydraulic diameters in the range 325 μm to 1819 μm. The test section was tested with air and water. The pressure variation along the length of the channel was measured and the values beyond the entrance region were used to calculate the friction factors.

The results of experiments conducted with water in smooth channels were used to validate the experimental setup. Fig. 3 shows the results obtained with water plotted with the conventional Fanning factor ($f = f_{\text{Darcy}}/4$) calculated using the channel base (gap $= b$) for calculating the cross-sectional area for fluid flow. It can be seen that the data points lie considerably above the theoretical laminar flow line.

The same data shown in Fig. 3 is replotted in Fig. 4 using b_{cf} as the gap height in calculating the constricted flow hydraulic diameter $D_{h,\text{cf}}$. It can be seen that the data agrees to within less than 6% with the theoretical laminar flow friction factors. Similar results are obtained at different gap heights and with air as well.

It may also be noted from Figs. 3 and 4 that the transition from laminar to turbulent flow is seen to occur at Reynolds numbers well below 2300. The critical Reynolds number is

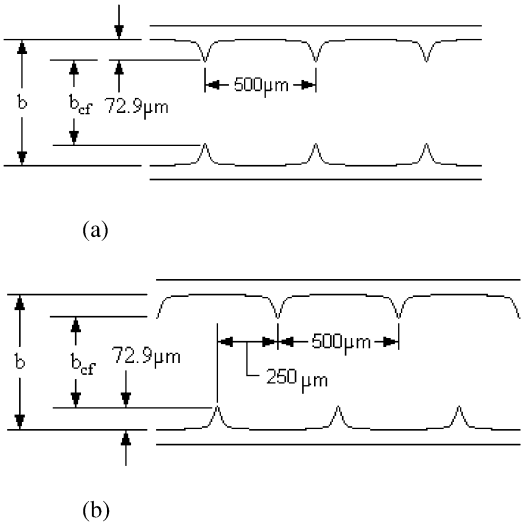

Fig. 2. Sawtooth roughness elements, (a) aligned sawtooth, and (b) offset sawtooth, studied by Kandlikar et al. [11] and Schmitt and Kandlikar [12].

therefore seen to depend on the relative roughness. Similar observations are made by a number of researchers in the literature.

3.2. Rising concerns in current systems

As the scale of systems continues to decrease, the need to revisit the impact and even the definition of roughness has arisen as shown in the previous section. The explosion of applications on the mini- and micro-levels has lead to some significant difficulties in execution, with at least some of those difficulties attributable to surface roughness concerns. One of the most telling problems has been that as the scale of the systems has decreased, the relative size of the roughness with respect to the pipe diameter has grown dramatically. Moody's original diagrams and method cannot accommodate relative roughness in

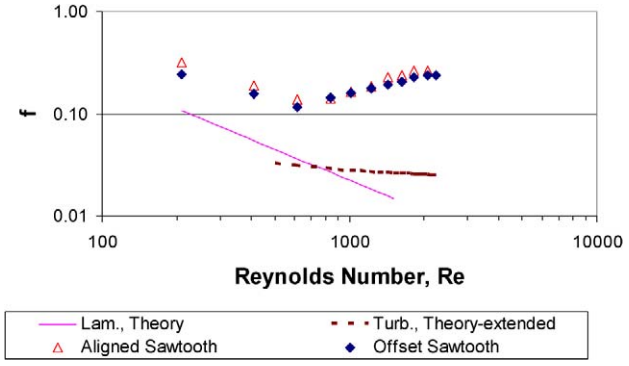

Fig. 3. Fully developed friction factor vs. Reynolds number, both based on hydraulic diameter; water flow. $D_h = 953$ μm, $b = 500$ μm, $b_{cf} = 354$ μm, $w = 10.03$ mm, $\varepsilon/D_h = 0.0735$.

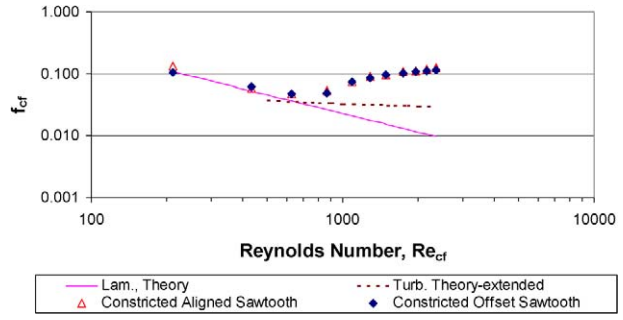

Fig. 4. Fully developed friction factor vs. Reynolds number, both based on constricted flow hydraulic diameter; airflow. $D_{h,cf} = 684$ μm, $b = 500$ μm, $b_{cf} = 354$ μm, $w = 10.03$ mm, $\varepsilon/D_{h,cf} = 0.1108$.

excess of 5%. The Moody diagram is simply the Colebrook [4] equation plotted over a wide range of Reynolds numbers and relative roughness values between 0 and 0.05. The diagram has served as an easy way to estimate the friction factor without performing a somewhat tedious calculation from the Colebrook equation. The laminar friction factor, as seen from the Moody's diagram, is independent of the relative roughness in the range $\varepsilon/D_t \leqslant 0.05$. In the turbulent region, the friction factor for smooth tubes continuously decreases with increasing Reynolds numbers. For rough tubes, the friction factor follows the smooth tube plot up to a certain point, and then approaches a higher asymptotic value (independent of the Reynolds number) depending on the relative roughness. The asymptotic value of the friction factor increases with relative roughness in the range $0 \leqslant \varepsilon/D_t \leqslant 0.05$. Relative roughness values routinely exceed that value in systems today. This lack of data has lead to renewed interest in the area and has forced the new experimentation presented in the previous section to be done. The accuracy of the data, based on the extrapolation of the Moody data has become more and more suspect, requiring the present work.

Recent work by Kandlikar et al. has explored systems with relative roughness values up to 14% for single phase fluid flow applications. To fully understand this data, six new roughness parameters have been proposed, three for roughness characterization (maximum profile peak height R_p, mean spacing of profile irregularities R_{sm}, and floor distance to mean line F_p),

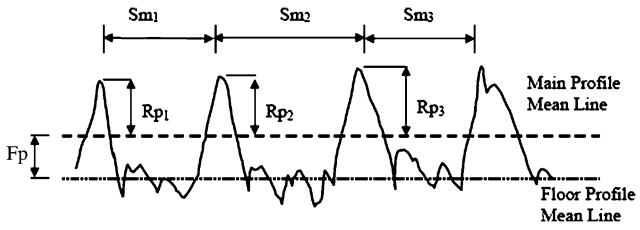

Fig. 5. Definition of roughness parameters.

and three for localized hydraulic diameter variation (maximum, minimum and average). The roughness ε is then defined as $R_p + F_p$.

Specific experiments were conducted using parallel sawtooth ridge elements, placed normal to the flow direction, in aligned and offset configurations in a 10.03 mm wide rectangular channel with variable gap (resulting hydraulic diameters of 325 μm to 1819 μm with *Re* from 200 to 7200 for air and 200 to 5700 for water). The use of constricted flow diameter extends the applicability of the laminar friction factor equations to relative roughness values up to 14%.

The newly proposed method requires the use of a more precisely defined roughness value and pipe diameter value to develop the relative roughness with which fluid flow practitioners are so familiar. Slight inaccuracies in the definitions that have been perpetuated from Nikuradse and in the current Moody diagram have been rather inconsequential up to this point because the relative roughness values have been so small. However, on the current mini- and micro-scales, systems have been dramatically affected by these inaccuracies in definition and significant departures from expected performance levels have been documented. The newly proposed definitions significantly improve the ability of the method to predict performance in regions that have not been documented to this point.

Measurement of the newly proposed roughness value is not a particularly difficult task given the use of modern profilometry. A standard roughness trace will produce ANSI/ASME (American National Standards Institute/American Society of Mechanical Engineers) standard parameters that can be used to generate the roughness value required for the analysis. The values of maximum profile peak height (R_p) and the floor distance to mean line of the profile (F_p) are simply added to generate the new roughness value ε. The floor profile mean line is the mean of all points on the surface that fall below the overall profile mean line. Fig. 5 shows a graphic representation of the parameters.

In addition to a more accurate representation of the roughness of the pipe walls, a more accurate representation of the pipe diameter is also warranted, again because of the more extreme relative roughness, the accuracy is much more important than in the past. The new method proposes to define the pipe diameter based on a constricted flow model using the previously calculated roughness parameter ε as shown in Eq. (2). Where D_t is the inner tube diameter that has typically been used in the past, modified by including the additional constricting effects of the roughness. The roughness factor is doubled because it is assumed to be present on both of the opposing walls of the pipe. If the surfaces on the two sides of the pipe, diametrically

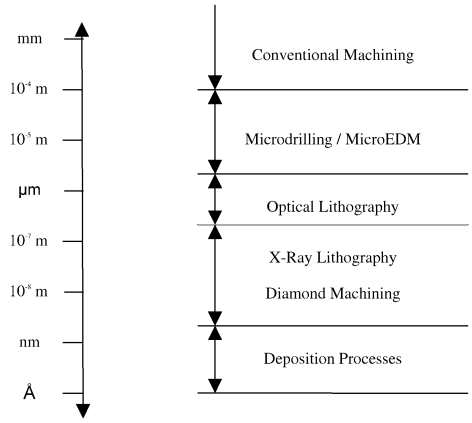

Fig. 6. Surfaces generated by various manufacturing processes.

opposed, are produced by different processes or are of different materials, the new diameter would be more accurately modeled by the following.

$$D_{\mathrm{cf}} = D_t - \varepsilon_1 - \varepsilon_2 \tag{6}$$

where ε_1 and ε_2 are the roughness values of the opposing wall of the pipe or channel.

The benefits of this new method have been shown in Schmitt et al. and include significantly improved modeling performance and an extension of the model into areas not covered previously. The limitations of the new method include some new measurement and analysis techniques that will need to be learned and incorporated and some issues with texture and alignment that are not addressed by the current method. The issues of texture are becoming more apparent as the size of systems becomes smaller. The methods of manufacture used to generate mini- and micro-channels produce characteristic roughness (see Fig. 6) as well as a surface pattern known as lay. This is typically generated by the interaction of the tools used with the surface and at a micro level is seen as a texture of repeated patterns on the surface. As hydraulic diameters decrease, the alignment of these textures from one surface to the other can have a significant impact on performance (see Schmitt and Kandlikar [12]), and yet would not be accounted in the proposed new model.

4. Future

The effect of relative surface roughness on friction factor in laminar and turbulent flow regions in relative surface roughness values beyond 0.05 is relevant in micro fluidics applications because of the small channel dimensions. Application of structured roughness surfaces may be employed to enhance heat and mass transfer processes. In order to develop accurate friction factor predictive models, experimental data is needed in the following regions.

(a) Laminar flow with uniform roughness for $\varepsilon/D_{h,\mathrm{cf}} > 0.05$.
(b) Laminar flow with different structured roughness surfaces by varying pitch, height, and three-dimensional shape of the roughness structures in the range $0 \leqslant \varepsilon/D_{h,\mathrm{cf}} \leqslant 0.15$ (the upper range of 0.15 is somewhat arbitrary, further understanding on the transport processes in the high relative roughness regions is expected to provide guidance).
(c) Turbulent flow region with uniform roughness for $\varepsilon/D_{h,\mathrm{cf}} > 0.05$.
(d) Turbulent flow region with structured roughness structures by varying pitch, height, and three-dimensional shape of the roughness structures in the range $0 \leqslant \varepsilon/D_{h,\mathrm{cf}} \leqslant 0.15$.
(e) Laminar to turbulent transition Reynolds number data for different roughness structures.

4.1. Future surface characterization methods for micro/mini-fluidic applications

In the quest for accurate functional correlations in surface measurement and analysis, the trends are basically leading into three distinct directions: a more effective use and assessment of 3D areial parameters, the use of new techniques such as length scale and areial scale fractal analysis, as well as the incorporation of new filtering techniques. In particular, the 3D surface assessment is anticipated to play an important role in metrology for surfaces in micro- and mini-channels.

Three-dimensional aerial parameters calculated from 3D topographical measurement data can explain functional correlations beyond roughness and waviness. Examples include wearability, lubricant retention, and angular direction of residual machining marks, among others. In the last ten years, significant effort has been directed towards developing standard 3D parameters. This has resulted in a set of standard "*S* parameters" divided into four general categories: amplitude, spatial, hybrid and functional.[1]

- *Amplitude parameters*: based on overall height. Some examples include: root mean square deviation (S_q), average of ten peaks and valleys (S_z), skewness (S_{sk}), kurtosis (S_{ku}), etc.
- *Spatial parameters*: based on frequency of features. Some examples include: density of summits (S_{ds}), texture aspect ratio (S_{tr}), fastest decay autocorrelation length (S_{al}), texture direction of surface (S_{td}), etc.
- *Hybrid parameters*: based on a combination of height and frequency. Some examples include: root mean square surface slope (S_{Dq}), mean summit curvature (S_{sc}), developed surface area ratio (S_{dr}), etc.
- *Functional parameters*: based on applicability for a particular function. Some examples include: surface bearing index (S_{bi}), core fluid retention index (S_{ci}), valley fluid retention index (S_{vi}).

Typical characterization of three-dimensional topography is achieved by means of height maps (Fig. 7) or intensity maps (Fig. 8).

Additionally, morphological filtering as well as length-scale and area scale fractal analysis may be the future methods of de-

[1] Not all of these categories are addressed by a single standard.

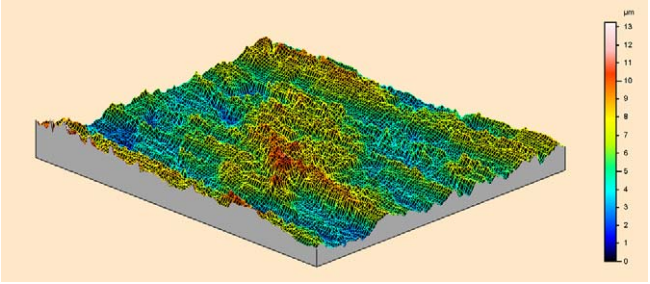

Fig. 7. Height map (Brown [13]).

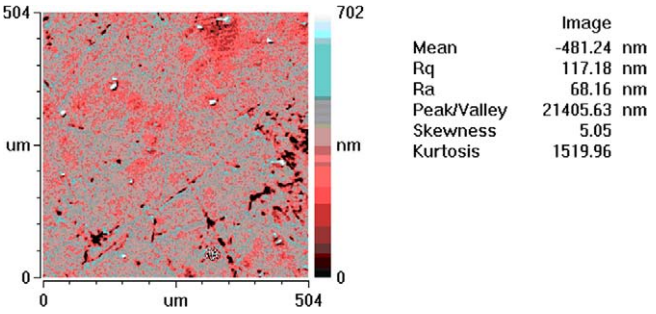

Fig. 8. Intensity maps (Carrano and Taylor [14]).

veloping accurate functional correlations for surfaces of micro- and mini-channels.

5. Conclusions

The future of mini- and micro-fluidics is clearly an unknown. Trends over the past 150 years would indicate that the scale of systems is going to continue to decrease in size, while being forced to increase in performance. With the decreasing scale of the systems, the relative importance of the roughness of the surface of the pipes (channels) is of increasing concern and effect. Pioneering work in this area over a century ago showed that roughness has a clear effect on the performance of fluid flow in networks and estimated that effect in a relatively simple, yet important way. The Moody diagram has served countless designers and engineers very well over the last many decades. More recently, the limitations of the Moody diagram have been brought to light, specifically as the relative roughness of systems has exceeded 5%. Current work in the area has modified the Moody diagram to accommodate the increased role of the relative roughness up to 14%, while accounting for the constricted flow effects of the mini- and micro-systems. This has been accomplished by the introduction of a new constricted flow diameter that more accurately reflects the conditions in mini- and micro-flow applications and the use of $F_p + R_p$ to more accurately reflect the roughness on the interior walls of the pipe (channel). Continuing to extrapolate the apparent trends would indicate that the scale of fluid systems will continue to decrease in the future and that the required performance will continue to increase. This leads to the inescapable conclusion that surface roughness is going to continue to play an increasingly important role in new fluid-based systems and technologies. The next step in understanding the effect of surface roughness on fluid flow will likely require the ability to understand, characterize and manipulate the surface in 3D. This 3D understanding of the surface and its interaction with the fluid flow will, not only lead to a more complete understanding of how the surfaces perform in practice, but will eventually lead to the ability to create designer surfaces to optimize system characteristics for heat transfer and other processes related to fluid flow networks. The scale of systems with improved performance and customization will give the opportunity to design systems for new applications in electronic, computing, biological, medical, space and other systems.

Acknowledgements

The authors would like to acknowledge the support of Kate Gleason College of Engineering, the Industrial and Systems Engineering Department, the Mechanical Engineering Department, and the students in the Thermal Analysis and Microfluidics Laboratory at RIT.

References

[1] H. Darcy, Recherches experimentales relatives au mouvement de l'Eau dans les Tuyaux, Mallet-Bachelier, Paris, 1857.
[2] J.T. Fanning, A Practical Treatise on Hydraulic and Water Supply Engineering, Van Nostrand, New York, 1877. Revised ed. 1886.
[3] J. Nikuradse, Laws of flow in rough pipes (Stromungsgesetze in Rauen Rohren), VDI-Forschungsheft, vol. 361, 1933. Beilage zu: Forschung auf dem Gebiete des Ingenieurwesens, Ausgabe B Band 4; English Translation NACA Tech. Mem. 1292, 1937.
[4] F.C. Colebrook, Turbulent flow in pipes, with particular reference to the transition region between the smooth and rough pipe laws, J. Inst. Civ. Engrg. London 11 (1939) 133–156.
[5] L.F. Moody, Friction factors for pipe flow, ASME Trans. 66 (1944) 671–683.
[6] ANSI/ASME B46.1-2002. Surface Texture (Surface Roughness, Waviness and Lay), American Society of Mechanical Engineers, 1995.
[7] ISO 4287: Geometrical Product Specifications (GPS) Surface Texture: Profile Method—Terms, Definitions and Surface Texture Parameters, 1997.
[8] H. Dagnall, Exploring Surface Texture, Rank Taylor Hobson Limited, Leicester, England, 1986.
[9] D.J. Whitehouse, Handbook of Surface Metrology, Institute of Physics Publishing, Bristol, 1994.
[10] S.G. Kandlikar, W.J. Grande, Evolution of microchannel flow passages—thermohydraulic performance and fabrication technology, Source Heat Transfer Engrg. 24 (1) (2003) 3–17.
[11] S.G. Kandlikar, D. Schmitt, A.L. Carrano, J.B. Taylor, Characterization of surface roughness effects on pressure drop in single-phase flow in minichannels, Phys. Fluids 17 (5) (2005).
[12] D. Schmitt, S.G. Kandlikar, Effects of repeating microstructures on pressure drop in rectangular minichannels, ASME Paper No. ICMM2005-75111, Third International Conference on Microchannels and Minichannels, Toronto, Canada, 2005.
[13] C.A. Brown, Applications of surface metrology in design, manufacturing and materials: diamonds, skis and potato chips, in: Graduate Seminar Series, Department of Industrial and Systems Engineering, Rochester Institute of Technology, October 2004.
[14] A.L. Carrano, J.B. Taylor, Geometric modeling of engineered abrasive processes, J. Manufacturing Processes Soc. Manufacturing Engrg. 7 (1) (2005) 17–27.